

# miR-500a-5p regulates oxidative stress response genes in breast cancer and predicts cancer survival

Davide Degli Esposti <sup>1</sup>, Vasily N. Aushev <sup>2</sup>, Eunjee Lee <sup>3</sup>, Marie-Pierre Cros <sup>1</sup>, Jun Zhu <sup>3</sup>, Zdenko Herceg <sup>1</sup>, Jia Chen <sup>4</sup>, Hector Hernandez-Vargas <sup>1</sup>

1. Epigenetics Group. International Agency for Research on Cancer (IARC), 150 Cours Albert-Thomas, 69008 Lyon, France.
2. Department of Environmental Medicine and Public Health, Icahn School of Medicine at Mount Sinai, New York, NY 10029, United States of America.
3. Department of Genetics and Genomic Sciences, Icahn Institute of Genomics and Multiscale Biology. New York, NY 10029, United States of America.
4. Department of Environmental Medicine and Public Health, Icahn School of Medicine at Mount Sinai, New York, NY 10029, United States of America. Department of Pediatrics, Icahn School of Medicine at Mount Sinai, New York, NY 10029, United States of America. Department of Medicine, Hematology and Medical Oncology, Icahn School of Medicine at Mount Sinai, New York, NY 10029, United States of America. Department of Oncological Sciences, Icahn School of Medicine at Mount Sinai, New York, NY 10029, United States of America.

## Supplementary Figures

### Figure S1. miR-500a-5p targets in two breast cancer cell lines.

Mir-500a-5p expression was modulated in MCF-7 and T47D cells by transfection of mimic and inhibitor. **a.** multidimensional scaling (MDS) of the normalized gene expression data was performed separately for MCF-7 (left panel) and T47D cells (right panel). Compare with the combined MDS plot shown in Figure 2b. **b.** 413 differentially expressed genes (DEGs) were obtained by comparing mimics vs. inhibitor in a linear regression model, and used for unsupervised clustering (left panel) and MDS plot (right panel). **c.** The same panel of 413 probes was used again for MDS plots separately for each cell line.

### **Figure S2. Target prediction with different algorithms.**

**a.** Similar to Fig 2f, we searched for the overlap between our list of experimental targets (“Targets”) and the targets predicted by miRDB (“miRDB”). In addition, we used the miRecords web tool which combines several target prediction algorithms<sup>32</sup>. For miR500a-5p we found a highly variable number of targets: RNAhybrid = 32724, PITA = 7251, miRanda = 3836, and miRtarget2 = 526. Of these, only 306 are common (corresponding to 236 annotated genes). The Venn diagram shows the overlap between these 236 genes (“miRecords”) with “miRDB” and our identified “Targets”. The overlap between our target list and miRecords is highly significant ( 7.6 times more than expected by chance, hypergeometric test p value < 1.095x10<sup>-19</sup>) using a conservative estimate of annotated human genes (20K). **b.** we tested for miRNA enrichment in our gene expression dataset, using the webtool MiRonTOP<sup>13</sup>. The resulting plots compare all annotated human miRNAs and their relationship with the full expression dataset of our in vitro experiment. The x-axis represents the enrichment (fold change) in putative targets for a given miRNA relative to the DEGs list, while the y-axis indicates the significance of that relationship. Negative relationships (gene downregulation after miRNA overexpression) are shown in green, while positive relationships are shown in red. For this particular analysis, we used the complementarity of the seed sequence to define a gene as a miRNA target, either in the UTRs (left panel) or the coding sequence (right panel). The position of miR500a-5p is indicated in both panels.

### **Figure S3. Functional pathway analyses.**

We used the EnrichR<sup>28,29</sup> **(a)** and DAVID<sup>30</sup> **(b)** pathway/ontology tools to infer the functional role of the 369 identified targets of miR500a-5p (see Methods). Only the top categories are shown, ranked by their statistical significance.

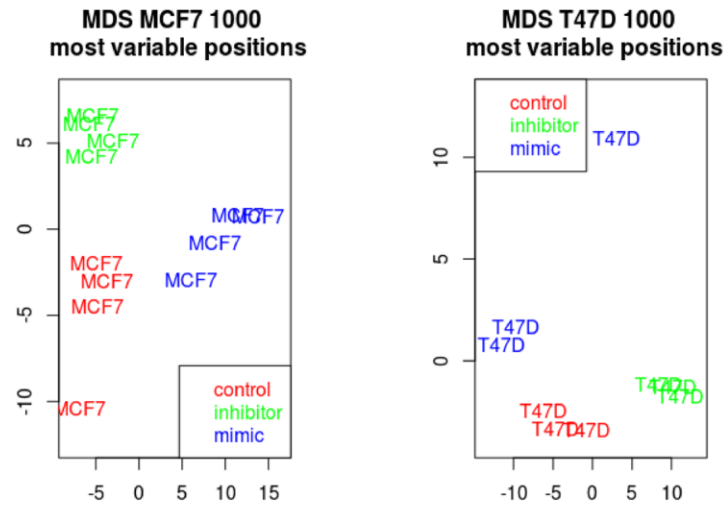
### **Figure S4. Survival analysis with identified miR-500a-5p targets (METABRIC dataset).**

The breast cancer dataset METABRIC was used to test for survival prediction capacity of miR-500a-5p oxidative stress targets (Table 1) in ER+ **(a)** ER- **(b)**, and ER-/HER2- **(c)** breast cancer samples. Cox regression model was used for each gene to predict relapse-free survival. The three most significant associations (lowest p values) are shown. Samples are divided into Low (black) and High (red) expression groups for each gene. Hazard ratio (HR) and P value for each association are shown within each plot.

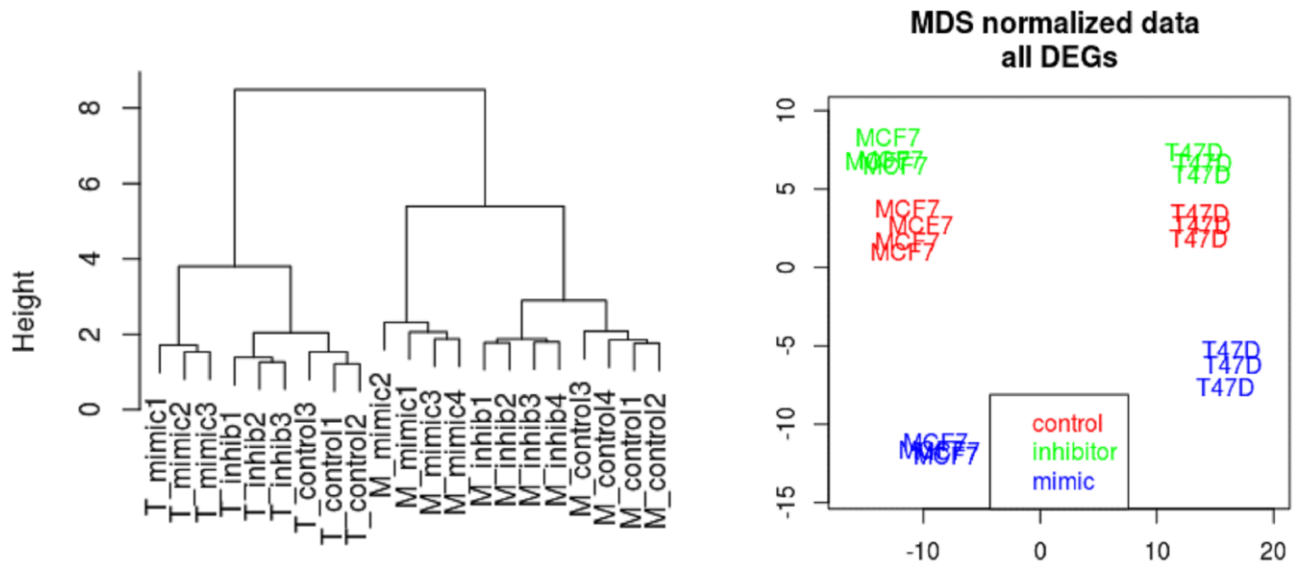
**Figure S5. Survival analysis with miR-500a-5p targets (KM Plotter dataset).**

The breast cancer dataset from Kaplan Meier Plotter (Gyorffy B. et al) was used to test for survival prediction capacity of miR-500a-5p oxidative stress targets (Table 1) in ER+ **(a)** ER- **(b)**, and ER-/HER2- **(c)** breast cancer samples. Cox regression model was used for each gene to predict relapse-free survival. Samples are divided into Low (black) and High (red) expression groups for each gene. Hazard ratio (HR) and P value for each association are shown within each plot.

**a**



**b**



**c**

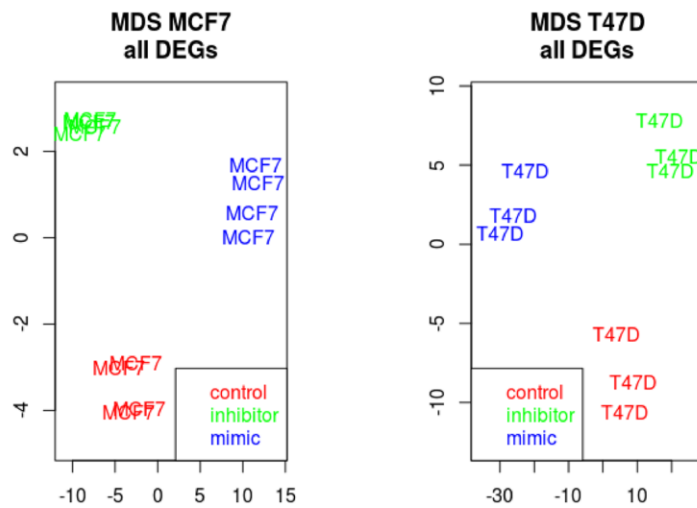
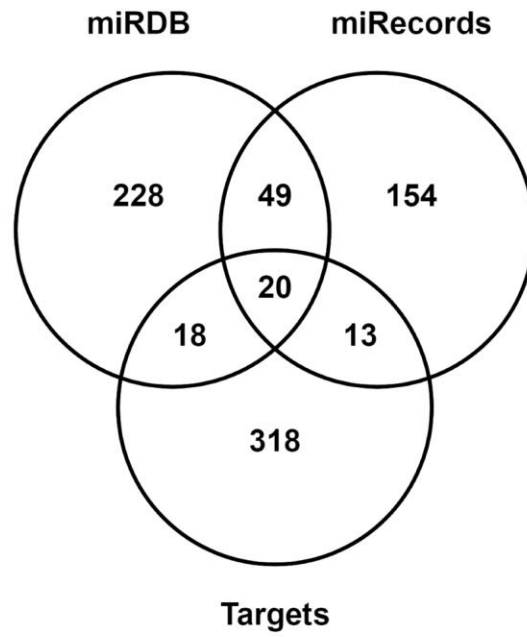


**Figure S1**

**a**



**b**

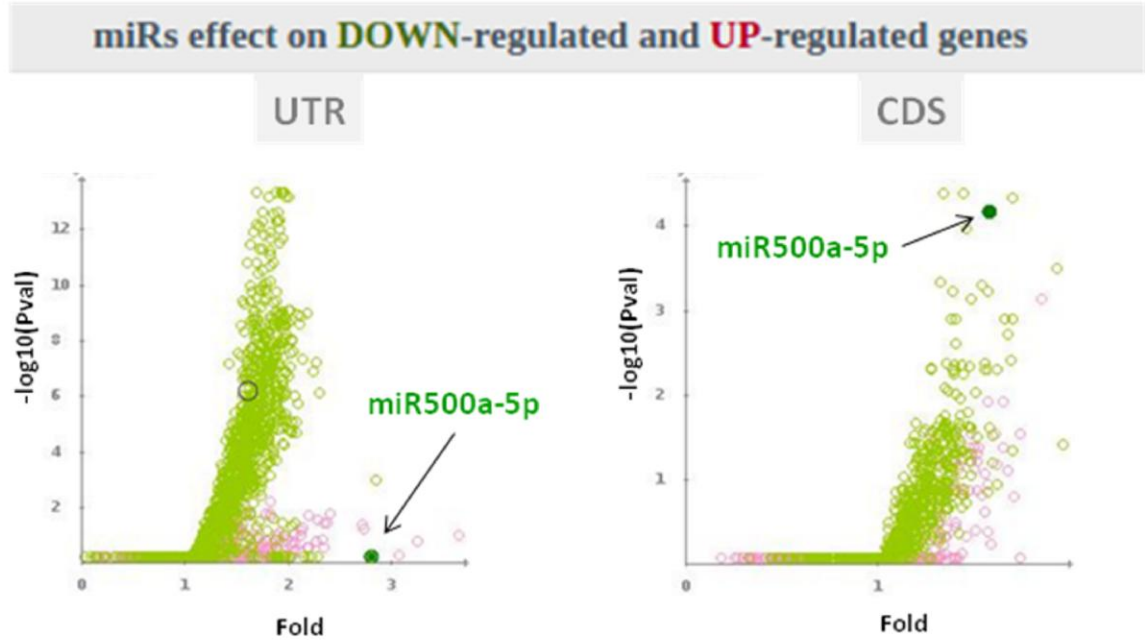


**Figure S2**

**a**

### KEGG 2016

Metabolic pathways\_Homo sapiens\_hsa01100  
 Pentose and glucuronate interconversions\_Homo sapiens\_hsa00040  
 Steroid hormone biosynthesis\_Homo sapiens\_hsa00140  
 Pentose phosphate pathway\_Homo sapiens\_hsa00030  
 Porphyrin and chlorophyll metabolism\_Homo sapiens\_hsa00860

### WikiPathways 2016

NRF2 pathway\_Homo sapiens\_WP2884  
 Oxidative Stress\_Homo sapiens\_WP408  
 Transcriptional activation by NRF2\_Homo sapiens\_WP3  
 Selenium Micronutrient Network\_Homo sapiens\_WP15  
 Keap1-Nrf2\_Mus musculus\_WP1245

### BioCarta 2016

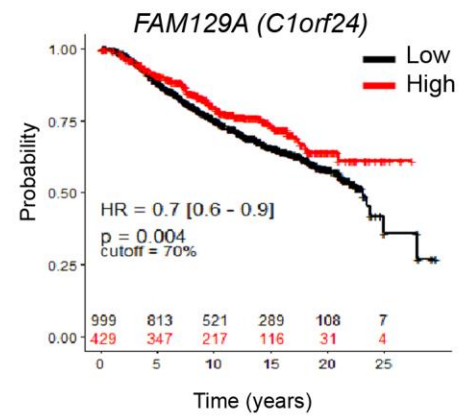
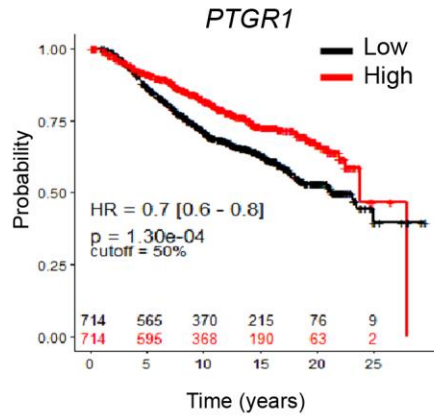
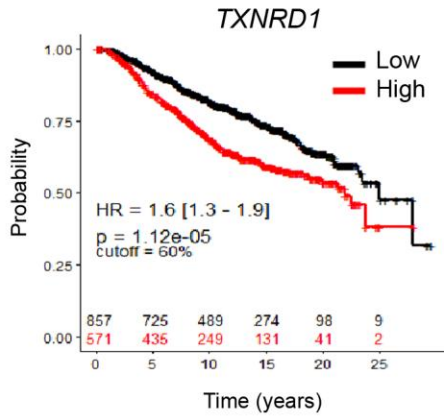
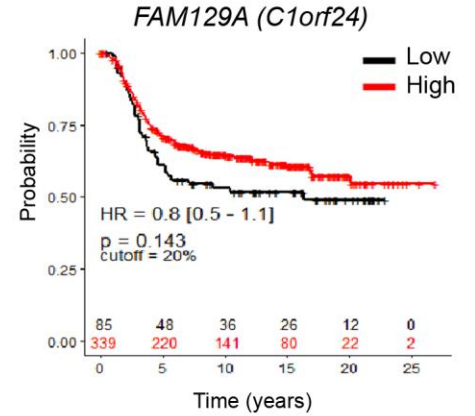
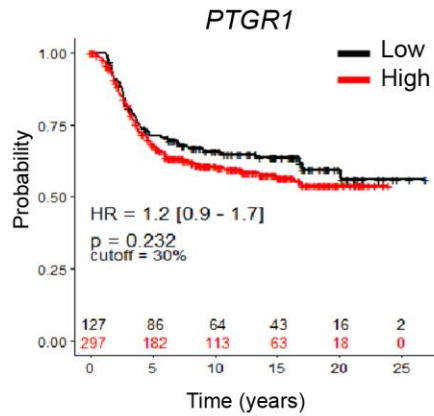
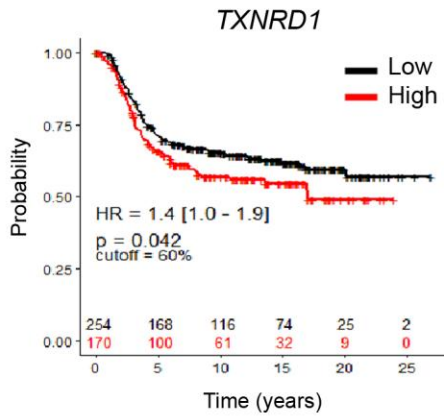
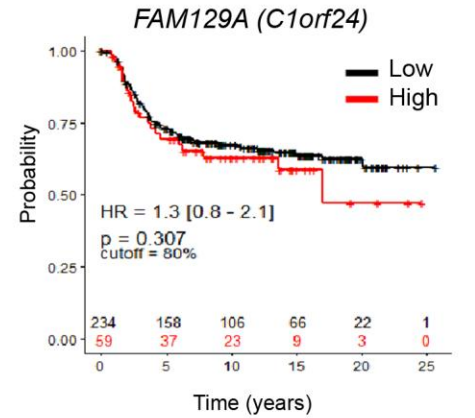
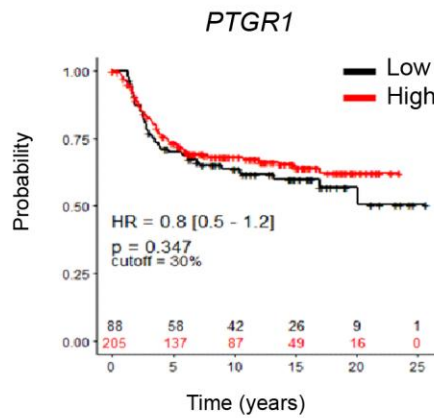
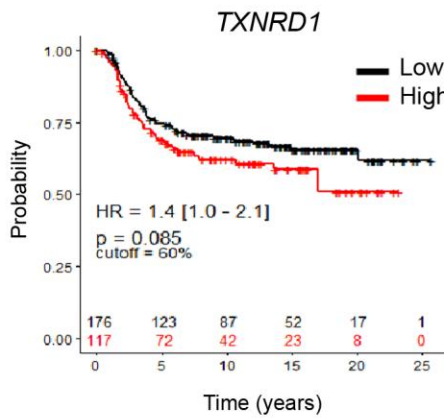
Oxidative Stress Induced Gene Expression Via Nrf2\_Homo sapiens\_h\_arenrf2Pathway  
 ER-associated degradation (ERAD) Pathway\_Homo sapiens\_h\_eradPathway  
 Caspase Cascade in Apoptosis\_Homo sapiens\_h\_caspasePathway  
 Skeletal muscle hypertrophy is regulated via AKT/mTOR pathway\_Homo sapiens\_h\_igf1mtorpathway  
 Role of Parkin in Ubiquitin-Proteasomal Pathway\_Homo sapiens\_h\_parkinPathway

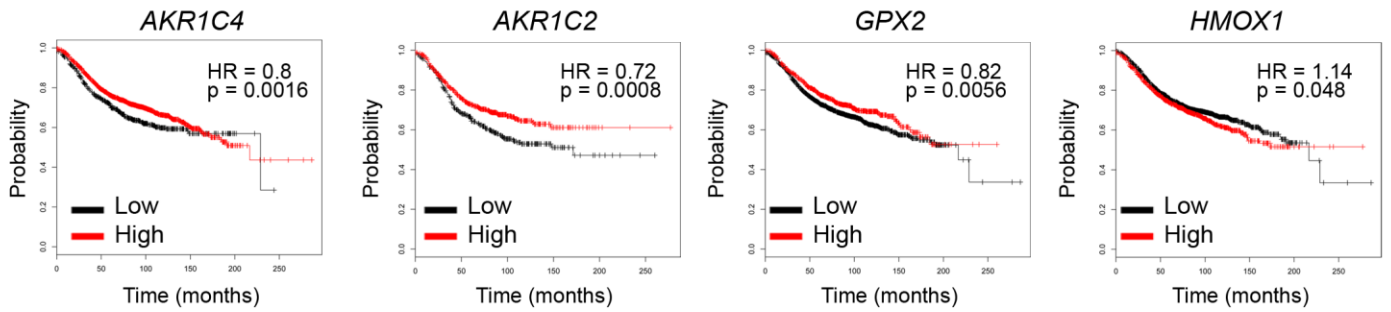
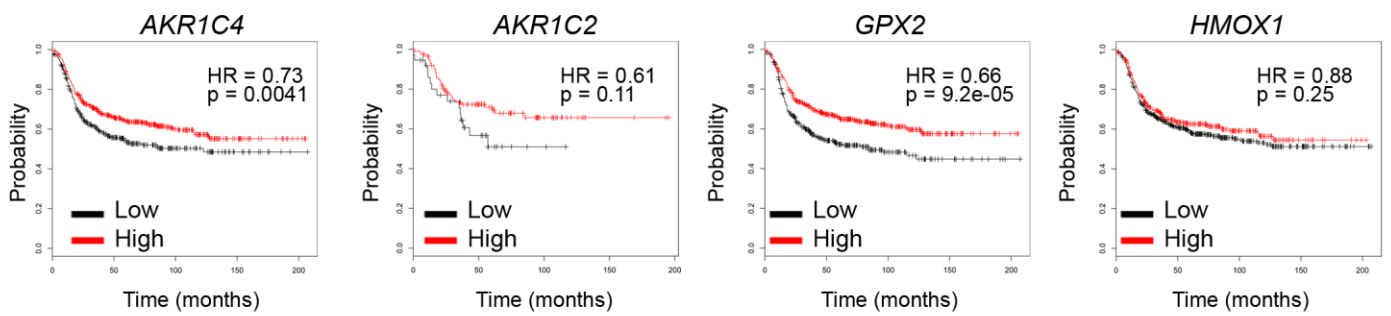
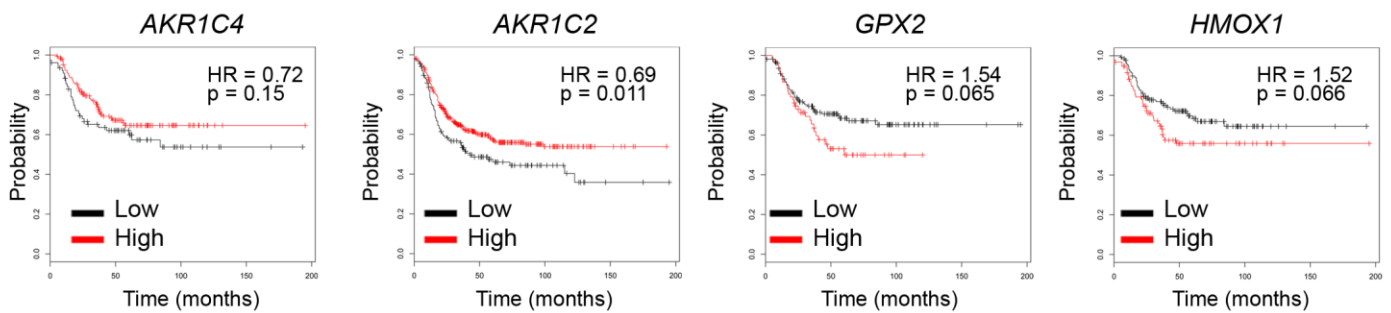
**b**

### Functional Annotation Clustering

Enrichment Score: 7.02		<b>G</b>	Count	P_Value	Benjamini
<a href="#">oxidation-reduction process</a>	<a href="#">RT</a>		36	7.5E-12	1.1E-8
<a href="#">Oxidoreductase</a>	<a href="#">RT</a>		30	1.8E-9	2.6E-7
<a href="#">NADP</a>	<a href="#">RT</a>		17	5.4E-9	5.3E-7
nucleotide phosphate-binding region:NADP	<a href="#">RT</a>		12	5.7E-9	4.5E-6
binding site:NADP	<a href="#">RT</a>		7	2.4E-6	9.5E-4
<a href="#">oxidoreductase activity</a>	<a href="#">RT</a>		13	6.5E-5	3.2E-2
binding site:Substrate	<a href="#">RT</a>		13	1.1E-3	1.9E-1

**Figure S3**

**a****ER Positive - Relapse-free survival****b****ER Negative - Relapse-free survival****c****ER Negative / HER2 negative - Relapse-free survival****Figure S4**

**a****ER Positive - Relapse-free survival****b****ER Negative - Relapse-free survival****c****ER Negative / HER2 negative - Relapse-free survival****Figure S5**